Width of bound eta in nuclei

H. C. Chiang* and E. Oset
Departamento de Física Teòrica and Instituto de Física Corpuscular, Centro Mixto Universidad de Valencia—Consejo Superior de Investigaciones Científicas, Facultad de Física, Burjassot (Valencia), Spain

L. C. Liu
Theoretical Physics, Los Alamos National Laboratory, Los Alamos, New Mexico 87545
(Received 22 June 1990)

Assuming the ηN interaction is dominated by the $N^*(1535)$ excitation we evaluate an η-nucleus optical potential that takes into account the free decay modes of the N^* plus its many-body decay modes up to one-particle-hole excitation. The potential is able to generate bound states in light and heavy nuclei but provides large widths for these states. The results are highly sensitive to the value of $\mathrm{Re}\Sigma_{N^*}$. In general, the widths are larger than the separation between the levels, although for $\mathrm{Re}\Sigma_{N^*}$ sufficiently repulsive a few narrow states can be found. In connection with a recent experiment our results suggest a potential for the N^* more attractive than for nucleons.

I. INTRODUCTION

It has been suggested that the ηN interaction is sufficiently attractive to support bound states of the η in nuclei [1–3]. The question arises of what is the width of these states. In Refs. [2,3] the widths of some η states were calculated and found to be narrow enough to be observable in principle, i.e., the sum of half-widths of two neighboring states would be smaller than the difference between the binding energies. Some searches for these states have led to negative results [6], while in a recent coincidence experiment, a broad bump in the region corresponding to bound etas is observed [7].

We have reanalyzed the problem by using a model that has a minimum amount of theoretical assumptions and, at the same time, is consistent with the known phenomenology of baryon decays. We have also considered the many-body modes of η decay in the nucleus involving η annihilation on two nucleons. These modes contribute to the imaginary part of the N^* self-energy, which we can determine rather reliably. On the other hand, we do not have enough information to undertake the evaluation of the real part. Hence we have varied it between reasonable limits. The η potential is found to vary appreciably with the value of $\mathrm{Re}\Sigma_{N^*}$, but the widths of the bound states are generally larger than the separation between the levels. However, for $\mathrm{Re}\Sigma_{N^*}$ sufficiently repulsive one can obtain a few narrow states.

II. THE MODEL

The first basic fact of phenomenology that we take into account is that, in the region of relevance to the problem, the $\eta(0^-)$, $N(\frac{1}{2}^+)$ system couples practically only to the N^* (1535; $\frac{1}{2}^-$) resonance, because about 50% of its width comes from decay into the $N\eta$ channel, while the branching ratio for the ηN channel in the decay of other N^* resonances, up to the $N^*(1700)$, is about or less than 1%. Hence we take the N^* (1535) pole, depicted in Fig. 1, as the dominant term in the $\eta N \to \eta N$ amplitude. With the quantum numbers of the particles involved the coupling $\eta N N^*$ is given by [1,2]

$$\delta H_{\eta N N^*}(x) = g_\eta \bar{\psi}_{N^*}(x)\psi_N(x)\Phi_\eta(x) + \mathrm{H.c.} \tag{1}$$

The η self-energy in nuclear matter, Π, is then given by the many-body diagram of Fig. 2 in analogy to the Δ-hole model for π-nucleus interaction [8]. We have

$$\Pi(k) = g_\eta^2 4 \int \frac{d^3p}{(2\pi)^3} n(\mathbf{p}) \times \frac{1}{\sqrt{s} - M_{N^*} + i[\Gamma(s)/2] - \Sigma_{N^*}(k^0+p^0, \mathbf{k}+\mathbf{p})}, \tag{2}$$

with $n(\mathbf{p})$ the occupation number in the Fermi sea, M_{N^*} the mass of the N^* (1535), $\Gamma(s)$ its free-space width, and Σ_{N^*} the N^* self-energy in the nuclear medium. The kinematical variables are $k^0 = \omega_\eta(\mathbf{k})$, the η energy, $\mathbf{k} \equiv \mathbf{k}_\eta$,

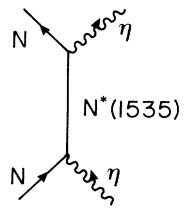

FIG. 1. Model for $\eta N \to \eta N$ amplitude through coupling to the N^* (1535).

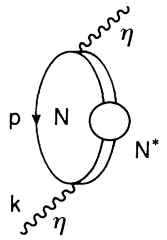

FIG. 2. Diagrammatic representation of the η self-energy in the nucleus through N^*-hole excitation. The circle in the N^* stands for the N^* self-energy.

and $p^0=\varepsilon_N(\mathbf{p})$, the nucleon kinetic energy. In the static limit for the nucleons, before the N self-energy is included, we have for the s variable

$$s=[M+\omega_\eta(\mathbf{k})]^2-\mathbf{k}^2 \ . \tag{3}$$

The evaluation of the real part of Σ_{N^*} is hardly possible at the present stage since it is equivalent to solving the problem of the N^*N interaction, for which no experimental information is available (recall that $\Sigma_{N^*}=t_{N^*N}\rho_N$ in the low-density limit, with t_{N^*N} the t matrix for N^*N interaction).

We then assume $\mathrm{Re}\Sigma_{N^*}$ to be of the type

$$\mathrm{Re}\Sigma_{N^*}=(\rho/\rho_0)V_{N^*} \ . \tag{4}$$

At the same time we will also include a nucleon self-energy that we take as

$$\mathrm{Re}\Sigma_N=(\rho/\rho_0)V_N \quad (V_N=-50\ \mathrm{MeV}) \ . \tag{5}$$

Since V_{N^*} is unknown we will vary V_{N^*}, within reasonable limits, to study its effect on the width of the η. The dependence of $\mathrm{Im}\Sigma_{N^*}(k^0+p^0,\ \mathbf{k}+\mathbf{p})$ on the energy and momentum of the nucleons is found to be sufficiently smooth in our calculations and can be neglected to a good approximation. We will then write from now on $\mathrm{Im}\Sigma_{N^*}(k^0,\mathbf{k})$.

Then the η self-energy can be written as

$$\Pi(k)=g_\eta^2\rho\frac{1}{\sqrt{s}-M_{N^*}+i[\Gamma(s)/2]-i\ \mathrm{Im}\Sigma_{N^*}(k^0,\mathbf{k})+\mathrm{Re}\Sigma_N-\mathrm{Re}\Sigma_{N^*}} \ , \tag{6}$$

where ρ is the nuclear density and $\mathrm{Im}\Sigma_{N^*}(k^0,\mathbf{k})$ is the imaginary part of Σ_{N^*}, which, as we shall see, can be calculated rather reliably using empirical information on the N^* decay channels.

III. THE N^* FREE WIDTH

We quote below the data from the compilation of particle properties [9] (the mean values suggested in the reference are inside brackets)

N^*mass: 1520 to 1560(1535) [MeV]
width: 100 to 250(150) [MeV]

partial decay modes:

$$\begin{aligned} &N\pi\ 35\text{–}50\,\% \ , \quad \text{we take } 40\% \ , \\ &N\eta\ 45\text{–}55\,\% \ , \quad \text{we take } 50\% \ , \\ &N\pi\pi\sim 10\% \ , \quad \text{we take } 10\% \ , \end{aligned} \tag{7}$$

$$\frac{\Gamma}{2}=75\ \mathrm{MeV}\begin{cases} 30\ \mathrm{MeV}\ N\pi \ , \\ 37.5\ \mathrm{MeV}\ N\eta \ , \\ 7.5\ \mathrm{MeV}\ N\pi\pi \ . \end{cases}$$

We must determine the energy dependence of the width, for which we need the coupling of the N^* to $N\pi$ and to $N\pi\pi$, in addition to the $N\eta$ given in Eq. (1). The coupling $N^*N\pi$ is given [1,2] by

$$\delta H_{\pi NN^*}(x)=g_\pi\bar{\psi}_{N^*}(x)\Phi(x)\tau\psi_N(x)+\mathrm{H.c.} \tag{8}$$

For the $N^*N\pi\pi$, accounting for 10% of the width, we choose not to make an elaborate model, but take the energy dependence from phase space. We accomplish that by taking a coupling of the type

$$\delta H_{N^*N\pi\pi}(x)=-iC\bar{\psi}_{N^*}(x)\gamma_5\psi_N(x)\Phi(x)\Phi(x)+\mathrm{H.c.} \ , \tag{9}$$

where the structure of the different mechanisms leading to the $N\pi\pi$ decay is accounted for by means of the effective coupling constant C.

In order to evaluate the width corresponding to these decay channels we calculate the N^* self-energy associated with the diagrams of Fig. 3 and use the relationship

$$\frac{\Gamma}{2}=-\mathrm{Im}\Sigma \ . \tag{10}$$

Thus for $N^*\to N\eta$ decay, Fig. 3(a), we find the c.m. system

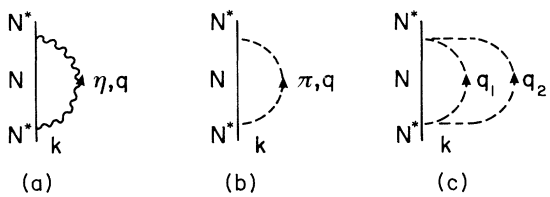

FIG. 3. Mechanisms contributing to the width of the N^*. (a) $N^*\to N\eta$; (b) $N^*\to N\pi$; (c) $N^*\to N\pi\pi$.

$$-i\Sigma=\int\frac{d^4q}{(2\pi)^4}g_\eta^2\frac{M}{E(\mathbf{k}-\mathbf{q})}\frac{1}{\sqrt{s}-q^0-E(\mathbf{k}-\mathbf{q})+i\epsilon}\times\frac{1}{q^{0^2}-\mathbf{q}^2-m_\eta^2+i\epsilon} \tag{11}$$

with $E(\mathbf{p})$ the nucleon relativistic energy. By using Cutkosky rules [10] [$\Sigma\to 2i\,\mathrm{Im}\Sigma$, $G(p)\to 2i\Theta(p^0)\mathrm{Im}G(p)$, $D(q)\to 2i\Theta(q^0)\mathrm{Im}D(q)$, with $G(p)$ and $D(p)$ the nucleon and η propagator of Eq. (11)] we have, finally,

$$\frac{\Gamma^{(\eta)}}{2}=\frac{g_\eta^2}{4\pi}\frac{M}{\sqrt{s}}\bar{q},\quad \text{for } N\eta \text{ decay}. \tag{12}$$

Analogously,

$$\frac{\Gamma^{(\pi)}}{2}=3\frac{g_\pi^2}{4\pi}\frac{M}{\sqrt{s}}\bar{q}',\quad \text{for } N\pi \text{ decay}, \tag{13}$$

where the extra factor 3 comes from the isospin counting and

$$\bar{q}=\frac{\lambda^{1/2}(s,M^2,m_\eta^2)}{2\sqrt{s}},\qquad \bar{q}'=\frac{\lambda^{1/2}(s,M^2,m_\pi^2)}{2\sqrt{s}}, \tag{14}$$

with $\mathbf{q},\mathbf{q}'$ being, respectively, the η and π momentum, given be the decay of an object of mass $\sqrt{s}$ in its c.m. frame, and $\lambda(x,y,z)$ the Källen function. The width for the $N\pi\pi$ decay channel is given in terms of Eq. (9) by

$$-i\Sigma(k)=i\int\frac{d^4q_1}{(2\pi)^4}\int\frac{d^4q_2}{(2\pi)^4}6\left[\frac{C}{4m_{\rm red}}\right]^2\mathbf{q}^2\frac{1}{(q_1^0)^2-\mathbf{q}_1^2-m_\pi^2+i\epsilon}\times\frac{1}{(q_2^0)^2-\mathbf{q}_2^2-m_\pi^2}\frac{M}{E(\mathbf{k}-\mathbf{q}_1-\mathbf{q}_2)}\frac{1}{\sqrt{s}-q_1^0-q_2^0-E(\mathbf{k}-\mathbf{q}_1-\mathbf{q}_2)+i\epsilon}, \tag{15}$$

with $m_{\rm red}$ the reduced mass of the NN^* system and $\mathbf{q}=\mathbf{q}_1+\mathbf{q}_2$. Using Eq. (10) and applying Cutkosky rules to Eq. (15), we obtain

$$\frac{\Gamma^{(2\pi)}}{2}=6\left[\frac{C}{4m_{\rm red}}\right]^2\frac{1}{4}\frac{M}{(2\pi)^3}\int_{m_\pi}^{\omega_{\max}}d\omega_2\,,\quad \int_{m_\pi}^{\sqrt{s}-M-\omega_2}d\omega_1[(\sqrt{s}-\omega_1-\omega_2)^2-M^2]P(\omega_1,\omega_2)\,, \tag{16}$$

where

$$P(\omega_1,\omega_2)=\begin{cases}1, & \text{if } \left|\frac{1}{2q_1q_2}[s+2m_\pi^2-M^2-2\sqrt{s}(\omega_1+\omega_2)+2\omega_1\omega_2]\right|\le 1\,,\\ 0, & \text{otherwise}\,,\end{cases}$$

$$\text{with } q_{1,2}=(\omega_{1,2}^2-m_\pi^2)^{1/2} \text{ and } \omega_{\max}=\frac{s-M^2-2Mm_\pi}{2\sqrt{s}}. \tag{17}$$

The factor 6 in Eq. (15) comes from isospin. A comparison of Eqs. (12), (13), and (16) with the numerical results of Eq. (7) at $\sqrt{s}=M^*=1535$ MeV provides the values of the coupling constants

$$g_\eta=2.06,\quad g_\pi=0.664\,,\quad C=9.23m_\pi^{-1}\,. \tag{18}$$

With this set of coupling constants one obtains only a rough agreement with the $\pi^-p\to\eta N$ reaction. We have varied the values of M_{N^*}, Γ_{N^*} and the decay branching ratios within the experimental uncertainties in order to obtain a good reproduction of the experimental $\pi^-p\to\eta n$ cross section [11]. Within the $N^*(1535)$ dominance model we use, the amplitude for this process is given by the diagram in Fig. 1, replacing the lower η by one pion. The cross section for this process in the c.m. system is readily evaluated, and we obtain

$$\frac{d\sigma}{d\Omega}=\frac{1}{16\pi^2}M^2 2g_\pi^2g_\eta^2\frac{q}{k}\frac{1}{s}\frac{1}{(\sqrt{s}-M_{N^*})^2+(\Gamma/2)^2}\,, \tag{19}$$

with q,k the eta and the pion momenta, respectively.

A fair reproduction of the cross section at $\sqrt{s}=1511$, 1542, and 1572 MeV is obtained if one takes $M_{N^*}=1555$ MeV, $\Gamma=110$ MeV, which are close, respectively, to the upper and lower bounds of the experimental values. Obviously the model provides only an s-wave contribution, but the experimental data are also smooth functions of the angle. One has to repeat now the steps used after Eq. (12), and we obtain new values for the coupling constants

$$g_\pi=0.564,\quad g_\eta=1.613,\quad C=7.14m_\pi^{-1}\,. \tag{20}$$

With these values the cross sections that we obtain for $\pi^-p\to\eta n$ are $d\sigma/d\Omega=0.118$, 0.219, and 0.198 mb/sr

for $\sqrt{s}=1511$, 1542, and 1572 MeV, respectively, which compare favorably with the experimental data of Ref. [11].

With a fair control of this reaction, the model provides the correct low-density limit [12], $[\Pi=t_{\eta N\to\eta N}(\mathbf{k},\mathbf{k})\rho]$ for the imaginary part of the η self-energy coming from the dominant channel $\eta N\to\pi N$. We also changed the branching ratios of Eq. (7) within the experimental limits, but the results are very stable; hence we kept the same branching ratios as in Eq. (7) in the calculations.

IV. MANY-BODY DECAY CHANNELS OF THE N^*

A. Pauli blocking corrections

In the decay of the N^* in nuclear matter we have to care that the final nucleon momentum is above the Fermi momentum k_F. This would introduce corrections in the $N^*\to N\eta$ decay channel, but they can be safely neglected in the $N^*\to N\pi$ and $N^*\to N\pi\pi$ decay channels because of the smaller masses of the one- or two-pion system with respect to the η. However, in the case of the bound-state problem, the diagram of Fig. 3(a) will not give a contribution to Γ, because there is no phase space available for this decay with the energy brought by the nucleon and the η in the diagram of Fig. 2.

Hence Fig. 3(a) does not contribute, reducing the N^* free half-width from 75 to 37.5 MeV. The s dependence of the $N\pi$ and $N\pi\pi$ channels in Eqs. (13) and (16) further reduces it to 33.1 MeV for an η just bound.

B. N^* decay due to $N^*N\to NN$ reaction

By analogy to the Δ decay in pion nuclear problems (Fig. 4), where the pion can excite a particle-hole (ph) pair in the medium, and lead to the $\Delta N\to NN$ decay channel [Fig. 4(b)], that accounts for two-nucleon pion absorption [Fig. 4(c)], we can also introduce the $N^*N\to NN$ decay channels of Fig. 5, which give rise, by means of Eq. (6), to two-nucleon absorption mechanisms in the η nuclear problem, as depicted in Fig. 6.

We evaluate now these three new channels. The contribution of Fig. 5(a) in the framework of nonrelativistic kinematics is

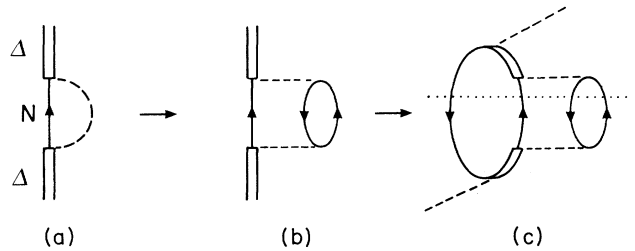

FIG. 4. Many-body diagrams in the Δ self-energy. (a) $\Delta\to N\pi$; (b) the π is allowed to interact with the medium exciting a ph. The mechanisms account now for $\Delta\to N$ ph; (c) corresponding diagram for the pion self-energy in the nucleus incorporating the mechanism (b) for the Δ self-energy. The mechanisms of (c) account for two-nucleon pion absorption.

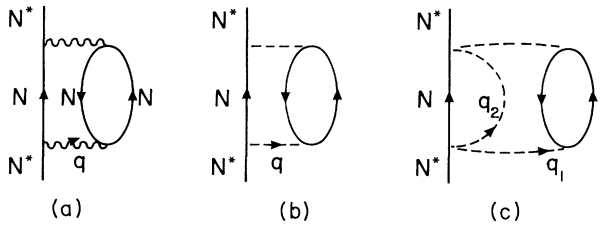

FIG. 5. Many-body diagrams for the N^* self-energy analogous to Fig. 4(b). (a) $N^*\to N$ ph driven by η exchange; (b) $N^*\to N$ ph driven by π exchange; (c) $N^*\to N$ ph π from $N^*\to N\pi\pi$ with one pion exciting a ph.

$$-i\Sigma(k^0,\mathbf{k})=\int\frac{d^4q}{(2\pi)^4}g_\eta^2\frac{1}{k^0-q^0-\epsilon(\mathbf{k}-\mathbf{q})+i\epsilon}D_\eta(q)^2\times\left[\frac{f_\eta}{m_\pi}\right]^2\mathbf{q}^2U_N(q)F_\eta^4(q)\ , \tag{21}$$

where $\epsilon(\mathbf{k}-\mathbf{q})$ is the nonrelativistic nucleon kinetic energy, $U_N(q)$ the Lindhard function for ph excitation [13] with the normalization of Ref. [14], and k^0, $\mathbf{k}$ the energy and momentum of the N^* (the origin of the energy is set here to the nucleon mass). We need an extra coupling, the ηNN, which is given by

$$\delta H_{\eta NN}(x)=-i\tilde{g}_\eta\bar{\psi}(x)\gamma_5\psi(x)\Phi(x) \tag{22}$$

in analogy to the πNN coupling

$$\delta H_{\pi NN}=-ig\bar{\psi}(x)\gamma_5\boldsymbol{\tau}\cdot\boldsymbol{\Phi}(x)\psi(x)\ . \tag{23}$$

Their respective vertex functions for mesons coming in with a momentum $\mathbf{q}$ are

$$\delta\tilde{H}_{\eta NN}=i\frac{f_\eta}{m_\pi}\boldsymbol{\sigma}\cdot\mathbf{q},\quad \delta\tilde{H}_{\pi NN}=i\frac{f}{m_\pi}\boldsymbol{\sigma}\cdot\mathbf{q}\tau^\lambda\ , \tag{24}$$

with $f_\eta/m_\pi=\tilde{g}_\eta/2M$, $f/m_\pi=g/2M$. In addition, we must add form factors of the type

$$F_i(q)=\left[\frac{\Lambda_i^2-m_i^2}{\Lambda_i^2-q^2}\right]\quad(i=\pi,\eta) \tag{25}$$

normalized to unity when the mesons are on shell. For simplicity we have assumed the same range for ηNN^*

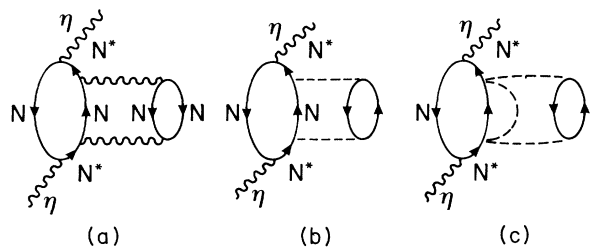

FIG. 6. Diagrams equivalent to the one in Fig. 4(c) contributing to the η self-energy in the nucleus and accounting for the corresponding pieces of the N^* self-energy of Fig. 5.

and ηNN vertices in Eq. (21). We use, from Ref. [15].

$$f_\eta = 0.59, \quad f = 1 ,$$
$$\Lambda_\eta = 1.5 \text{ GeV}, \quad \Lambda_\pi = 1.3 \text{ GeV} . \tag{26}$$

We also mention that, because a different expression of form factor was used in Ref. 1, the coupling constants of that work, denoted g', are related to those of Eqs. (18) and (20) by

$$g_i^2 = \alpha_i g_i'^2 [M\sqrt{s}/\omega_\eta(\mathbf{q})E_N(\mathbf{q})](1+\mathbf{q}^2/\Lambda' i^2)/(2\pi^2) ,$$

$i = \pi, \eta$ with $\alpha_\pi = 3$ and $\alpha_\eta = 1$. The Λi^2 is the range parameter given in Ref. [1].

The coupling constants are in agreement with those quoted in Ref. [16]. We can use again Cutkosky rules [adding $U(q) \to 2i\Theta(q^0)\mathrm{Im}U(q)$], and by means of the useful approximation [17]

$$\Theta(q^0)\mathrm{Im}U_N(q) \approx -\pi\rho\delta(q^0 - \mathbf{q}^2/2M) \tag{27}$$

we obtain

$$\frac{\Gamma^{(\eta,\mathrm{abs})}}{2} = \frac{g_\eta^2}{4\pi}\frac{f_\eta^2}{m_\pi^2}\rho M\tilde{q}^3 \left[\frac{1}{q^{02} - \tilde{q}^2 - m_\eta^2}\right]^2 F_\eta^4(q^0, \tilde{q}) .$$

Strictly speaking, our formulas in Eqs. (11) and (15) should also include a form factor. However, since we are only interested in the imaginary part of the self-energy which comes when the mesons are placed on shell, the form factor would be unity with our normalization. In Eqs. (2) and (6) we have the eta on shell and the form factor is also unity:

$$\tilde{q} = \sqrt{Mk^0 - \mathbf{k}^2/2} , \quad q^0 = \tilde{q}^2/2M . \tag{28}$$

Analogously, for the diagram of Fig. 5(b) we obtain

$$\frac{\Gamma^{(\pi,\mathrm{abs})}}{2} = 3\frac{g_\pi^2}{4\pi}\frac{f^2}{m_\pi^2}\rho M\tilde{q}^3 \left[\frac{1}{q^{02} - \tilde{q}^2 - m_\pi^2}\right]^2 F_\pi^4(q_0, \tilde{q}) , \tag{29}$$

with the same kinematics as in Eq. (28). The factor 3 comes from the pion isospin sum.

Finally, the diagram of Fig. 5(c) gives

$$-i\Sigma(k^0,k) = 2i\int \frac{d^4q_1}{(2\pi)^4}\int \frac{d^4q_2}{(2\pi)^4} 6\left[\frac{C}{4m_{\mathrm{red}}}\right]^2 (\mathbf{q}_1+\mathbf{q}_2)^2 D_\pi(q_1)^2 \frac{f^2}{m_\pi^2}\mathbf{q}_1^2 U_N(q_1)$$
$$\times D_\pi(q_2)\frac{1}{k^0 - q_1^0 - q_2^0 - \varepsilon(\mathbf{k}-\mathbf{q}_1-\mathbf{q}_2) + i\epsilon} F_\pi^4(q_1) , \tag{30}$$

where the factor 2 appears because the ph can be excited by either pion.

Using again Cutkosky rules and Eq. (27), placing on shell the pion with momentum q_2, the nucleon and the particle-hole excitation, we obtain from Eq. (30)

$$\frac{\Gamma^{(2\pi,\mathrm{abs})}}{2} = 6\frac{1}{(2\pi)^3}\frac{f^2}{m_\pi^2}\left[\frac{C}{4m_{\mathrm{red}}}\right]^2 \rho\int_0^{q_{2\max}} q_2\, dq_2 \int_0^{q_{1\max}} q_1\, dq_1 [2Mk^0 - q_1^2 - k^2 - 2M\omega(q_2)]\frac{M}{\omega(q_2)} q_1^2 F_\pi^4(q_1^0, q_1)$$
$$\times \left[\frac{1}{q_1^0 - q_1^2 - m_\pi^2}\right]^2 \Bigg|_{q_1^0 = q_1^2/2M} P_2(q_1,q_2) , \tag{31}$$

where $q_1 = |\mathbf{q}_1|$, $q_2 = |\mathbf{q}_2|$, $k = |\mathbf{k}|$, and $P_2(q_1,q_2)$ is a phase-space factor:

$$p_2(q_1,q_2) = \begin{cases} 1, & \text{if } \left|\dfrac{M}{q_1 q_2}\left[k^0 - \dfrac{k^2}{2M} - \dfrac{q_1^2}{M} - \dfrac{q_2^2}{2M} - \omega(q_2)\right]\right| < 1 , \\ 0, & \text{otherwise} , \end{cases} \tag{32}$$

Furthermore,

$$q_{2\max} = A^{1/2} ,$$
$$q_{1\max} = [q_2 + (A - q_2^2)^{1/2}]/2 , \tag{33}$$

and

$$A = 4Mk^0 - 2k^2 - 4Mm_\pi .$$

We have assumed for simplicity $k \ll q_1$, $k \ll q_2$, and put, like in Eq. (16), easy analytical integration limits instead of the strict ones. We also note that the phase factor eliminates the unphysical regions.

V. NUMERICAL RESULTS

For $k^0 = m_\eta$, $\sqrt{s} = M + m_\eta$, the choice of N^* mass and width of Eqs. (7) and the coupling constants of Eq. (18) we get

$$\frac{\Gamma^{\text{free}}_{(s)}}{2}=33.1\ [\text{MeV}]\ ,$$
$$\frac{\Gamma^{(\eta,\text{abs})}}{2}=1.35\rho/\rho_0\ [\text{MeV}]\ ,$$
$$\frac{\Gamma^{(\pi,\text{abs})}}{2}=4.41\rho/\rho_0\ [\text{MeV}]\ , \tag{34}$$
$$\frac{\Gamma^{(2\pi,\text{abs})}}{2}=29.12\rho/\rho_0\ [\text{MeV}]\ ,$$
$$\frac{\Gamma^{\text{abs}}_{\text{tot}}}{2}=34.88\rho/\rho_0\ [\text{MeV}]\ .$$

The many-body corrections give a width comparable to the free width at $\rho=\rho_0$. It might look curious that the contribution from the 2π absorption diagram is larger than the one from one-pion absorption, whereas for pions on shell $\Gamma^{(\pi)}>\Gamma^{(2\pi)}$. This is a consequence of phase space plus the additional counting factor of 2 and the fact that $(\mathbf{q}_1+\mathbf{q}_2)^2$ is larger in the case of 1π ph excitation than in the case of 2π on shell. A similar behavior has also been observed in the evaluations of the proton decay in nuclei [18] and in the many-body modes of antiproton decay in nuclei [19,20]. It is also worth mentioning that one should go ahead with the diagrams of Fig. 6, consider the ph excitation to be a contribution to the η or π self-energy, and then generate all the random-phase approximation diagrams. Taking into account this series of diagrams can lead to important corrections in the Δ self-energy for $k^0\simeq m_\pi$, Ref. [21]. However, as the energy increases the corrections become less important [22]; and for an energy $k^0=m_\eta$ they can be safely neglected.

The introduction of the $\Gamma^{\text{free}}/2$ and $\text{Im}\Sigma\equiv-\Gamma^{(\text{abs})}/2$ of Eq. (34) into Eq. (6) gives us the optical potential of an η particle in the nuclear matter. In order to obtain the optical potential in a finite nucleus we use the local-density approximation and substitute ρ by $\rho(\mathbf{r})$ with $\rho(\mathbf{r})$ being the proton density distributions, Ref. [23], after correcting for the finite proton size [24]. We further assume equal density distribution for protons and neutrons.

With this optical potential we calculate the bound states of the η in the nuclei ^{12}C, ^{40}Ca, ^{208}Pb in order to have the results for a sample of nuclei over the Periodic Table. We use the complex version [25] of the highly accurate method to solve the Schrödinger equation [26].

In order to have a feeling for the optical potential that

TABLE I. Bound states of η found for different nuclei and different assumptions on the potential. The first block assumes no medium renormalization of the N or N^*. The other three blocks consider $\text{Im}\Sigma_{N^*}$ evaluated in the text and three different choices of V_{N^*}(−50 MeV, 0, and 50 MeV, with $V_N=-50$ MeV). B is the binding energy and Γ the width of the state. The numbers in the second column of B and Γ correspond to the choice of $M_{N^*}=1555$ MeV and $\Gamma_{N^*}=110$ MeV.

$V_N-V_{N^*}$ [MeV]	Nucleus	n	l	B [MeV]		Γ [MeV]	
0 (and Im $\Sigma_{N^*}=0$)	^{12}C	1	0	26	9	82	18
	^{40}Ca	1	0	47	22	98	25
		1	1	24	5	83	18
	^{208}Pb	1	0	59	32	101	27
		1	1	51	25	97	26
		2	0	36	13	90	22
		2	1	22	3	84	18
0 (Im $\Sigma_{N^*}\neq0$)	^{12}C	1	0		8		19
	^{40}Ca	1	0	14	21	86	27
		1	1		4		19
	^{208}Pb	1	0	25	31	94	30
		1	1	18	24	90	28
		2	0	6	12	81	24
		2	1		1		20
−50 (Im $\Sigma_{N^*}\neq0$)	^{12}C	1	0	6	3	32	6
	^{40}Ca	1	0	18	11	42	10
		1	1	3		33	
	^{208}Pb	1	0	27	18	47	11
		1	1	21	13	44	10
		2	0	10	3	40	8
−100 (Im $\Sigma_{N^*}\neq0$)	^{12}C	1	0	5		16	
	^{40}Ca	1	0	14	6	23	5
	^{208}Pb	1	0	22	12	25	6
		1	1	16	7	24	5
		2	0	6		21	

we have, we write it down for $\rho=\rho_0$, $V_N=-50$ MeV, and several values of V_{N^*}, corresponding to $V_{N^*}=-50$, 0, and 50 MeV. We also show the results obtained without the many-body corrections (i.e., $\mathrm{Im}\Sigma_{N^*}=\mathrm{Re}\Sigma_N=\mathrm{Re}\Sigma_{N^*}=0$), which we denote as V_η^{free}.

Recalling that $2\omega V_\eta\equiv\Pi$, and Eq. (6), we obtain

$$V_\eta^{\mathrm{free}}(\rho_0)=(-70.45-i48.69)\ \mathrm{MeV}\ ,$$

$$V_\eta(\rho_0)=(-34.52-i49.01)\ \mathrm{MeV}\ ,\quad \text{for } V_{N^*}=-50\ \mathrm{MeV}\ ,$$

$$V_\eta(\rho_0)=(-34.36-i23.86)\ \mathrm{MeV}\ ,\quad \text{for } V_{N^*}=0\ \mathrm{MeV}\ ,$$

$$V_\eta(\rho_0)=(-27.79-i12.79)\ \mathrm{MeV}\ ,\quad \text{for } V_{N^*}=50\ \mathrm{MeV}\ , \tag{35}$$

Of course, the η particle does not feel exactly a density ρ_0, but something smaller. With the first two potentials we can expect η widths about 90–100 MeV. With the last one, we expect the width to be around 24 MeV [note that if the effective value of ρ decreases, $\mathrm{Im}V_\eta$ increases such that $\mathrm{Im}V_\eta(\rho_{\mathrm{eff}})\rho_{\mathrm{eff}}\simeq\mathrm{const}$].

It is interesting to see that for $V_N=V_{N^*}$ the inclusion of the absorption channels in the N^* width does not change much the imaginary part of V_η, with respect to V_η^{free}. However, it reduces appreciably the real part, making the potential less attractive. The resonant character of the optical potential [Eq. (6)] is responsible for it.

Energies and widths, calculated with the potential of Eq. (6), $\mathrm{Im}\Sigma$ of Eqs. (34) and the different choices of $\mathrm{Re}\Sigma_{N^*}$, are given in Table I. We also add the results given by the omission of the many-body corrections. In the case of ^{12}C and no medium modifications, we find only one bound state, which we denote $1s$. (Note that the principal quantum number n does not count the number of nodes, because here we have a complex potential. It only serves as a classification index ordering the levels as the energy in each partial wave l increases). For ^{40}Ca, we find two bound states: one with $l=0$ and the other with $l=1$, while in ^{208}Pb we find four: two with $l=0$ and two with $l=1$. The width of these states is very large, ranging from 82 to 100 MeV. In all cases the sum of half-widths for two neighboring states is much larger than the difference of energy between the levels (90 versus 10–25 MeV). This would make the identification of the individual states impracticable. For the case of medium corrections and assuming $V_{N^*}=-50$ MeV one loses the $1s$ state of ^{12}C, the $1p$ of ^{40}Ca, and the $2p$ in ^{208}Pb. This is a consequence of the fact that the real part of the attractive potential V_η is considerably reduced in size. One also sees that the binding energies are considerably reduced with respect to the former case. The widths are about 80–95 MeV, similar to those before, and they are much bigger than the separation of energies of about 7–13 MeV. The widths are very sensitive to the value assumed for V_{N^*}. The most favorable case for narrow η widths is given by $V_{N^*}=50$ MeV, repulsive instead of attractive and of the same strength (and opposite sign) as the nucleon potential. In this case the widths range from 16 to 25 MeV. However, even in this case these widths are much larger than the separation between the levels.

With the input parameters derived from $\pi^-p-\eta n$ cross sections we have recalculated the optical potential and the energies and widths of the new states. Corresponding to Eqs. (35) we now obtain

$$V_\eta^{\mathrm{free}}(\rho_0)=(-40.82-i14.00)\ \mathrm{MeV}\ ,$$

$$V_\eta(\rho_0)=(-31.89-i20.93)\ \mathrm{MeV}\ ,\quad \text{for } V_{N^*}=-50\ \mathrm{MeV}\ ,$$

$$V_\eta(\rho_0)=(-22.99-i8.69)\ \mathrm{MeV}\ ,\quad \text{for } V_{N^*}=0\ \mathrm{MeV}\ ,$$

$$V_\eta(\rho_0)=(-17.24-i4.57)\ \mathrm{MeV}\ ,\quad \text{for } V_{N^*}=50\ \mathrm{MeV}\ . \tag{36}$$

The values for the energies and widths appear in the second column of B and Γ in Table I, besides the results discussed above.

As a comparison of Eqs. (35) and (36) shows, the new potential is less attractive and has a smaller imaginary part. As a consequence, the states are less bound and have a smaller width than with the potential of Eqs. (35). We observe that the trend is, however, similar to the one before. The separation between the levels is in general smaller than the widths of the states. The most favorable case for narrow states appears at $V_{N^*}=50$ MeV. The two states in ^{208}Pb appear overlapped, but are separated about 4.5 MeV from the continuum. The bound state of ^{40}Ca is also separated by about 3.8 MeV from the continuum. However, we should also notice that this case is also the weakest case theoretically because by taking the 100-MeV difference between the binding of the N and the N^*, the pole in the propagator of Eq. (6) appears at $\sqrt{s}=1655$ MeV for $\rho=\rho_0$, or 170 MeV above the energy of the $N\eta$ system in the atoms studied. Because of that we can no longer claim dominance of the N^* pole. Other terms in the amplitude would now play a more important role. Also, below threshold, resonances like the N^* (1440) would provide a stronger weight to the optical potential, with a repulsive contributive which would unfavor the binding of the etas in the nucleus.

The other point worth mentioning is that in the wide range of cases studied, there is always an attraction on the η which allows this particle to be bound in nuclei even if with a large width. This would have as a consequence that, in the production of etas in nuclei, some of the strength would be collected below the continuum of the asymptotic eta nucleus system.

At this point it is interesting to make connection with the experimental work of Ref. [6]. In this work the (π,p) reaction on ^{16}O was measured and no appreciable enhancement was seen in the region where a peak had been predicted in Ref. [3]. The conclusion of the authors of Ref. [6] is that the height of the peak should be three times smaller than what had been predicted. This suggests that the width of the states is at least three times

bigger than what was used in Ref. [3] and hence Γ should be about 30 MeV or more. This would be compatible with the results of Table I provided the N^* potential is more attractive than the one of the nucleon. This seems to go in the opposite direction as the delta potential deduced from the studies of the delta hole model of Refs. [27–31]. Indeed, the studies with the phenomenological delta-hole models of Refs. [27–29] give a delta potential less attractive than the one of the nucleon. These pictures, however, use only pion exchange for the delta-hole interaction. Instead, the microscopic models of Ref. [30,31] include also the Landau-Migdal interaction in this channel, which has a repulsive character. It can be seen in Ref. [31] that the effect of the Landau-Migdal force can be simulated by adding a repulsive piece to the delta self-energy. This, in addition to a calculated attractive piece and to an attractive Hartree potential equal to the nucleon potential, leads to a delta potential less attractive than the one of the nucleon, in accordance with the results of the phenomenological models. However, the origin of the Landau-Migdal force lies in the p-wave character of the $\pi N\Delta$ coupling and this force is absent in the N^*-hole model we have developed here, because the N^* is an s-wave resonance. Hence, the analogy with the delta case would suggest a potential more attractive than the one of the nucleon.

VI. CONCLUSIONS

We have taken advantage of the strong coupling of the η to the $N^*(1535)$ in order to make a model for the $\eta N \to \eta N$ interaction. The evaluation of the η nucleus optical potential required the computation of the N^* self-energy in a nuclear medium. Using available empirical information we could evaluate rather reliably the imaginary part of Σ_{N^*}, but not the real part. Thus we evaluated the optical potential for several choices of V_{N^*} ranging from 50-MeV attraction to 50-MeV repulsion. We also evaluated the optical potential with two sets of values for the position and width of the N^*. The results for energies and widths depend strongly on the value of V_{N^*} and the mass and width of the N^*. For the case where the nucleon and N^* have the same binding, we find several bound states in medium and heavy nuclei. The widths are, however, very large, of the order of 25–80 MeV. For other choices of V_{N^*} the widths become smaller. Assuming a repulsive N^* potential with 50 MeV of strength the widths are about 20–25 MeV if average values for M_{N^*} and Γ are taken, or about 5 MeV if the choice leading to good $\pi N \to \eta N$ cross sections is taken. In the first case the widths are larger than the separation of energies, while in the second case, for nuclei like ^{40}Ca one obtains a bound state with a half-width smaller than the binding and hence, separated from the continuum. However, we also observed that this is a case where the dominance of the N^* pole no longer holds and other terms of repulsive character would become more important, thus reducing the binding of the η and the changes to have widths narrower than the separation between the levels. Thus, even with the present uncertainties we tend to conclude that it is rather unlikely that any narrow peaks, corresponding to bound eta states in nuclei, are detected experimentally. In this sense, the experimental results of Ref. [6], together with the theoretical analysis of Ref. [3], already suggest that the widths in a nucleus like oxygen are around 30 MeV or larger. This, according to the present study, would indicate that the N^* feels an attractive potential bigger than the one of the nucleon. Our calculations further indicate that there are bound states of eta in nuclei, which would pick up some of the strength in η-production reactions in nuclei even if with large decay widths.

The many-body study done here could be applied to the problem of propagation of η particles through nuclei. It is clear, however, that we need further information concerning mostly V_{N^*}. Experiments on η absorption could provide information on that magnitude since we have shown that there is a large sensitivity of $\mathrm{Im}V_\eta$ to the value of V_{N^*}. In addition, precise experiments searching for eta bound states could also provide more detailed information on that magnitude.

ACKNOWLEDGMENTS

This work was partly financed by the Spanish CICYT. One of us (H.C.C.) wishes to acknowledge the Spanish Ministry of Education for support in a sabbatical stay at Valencia and L.C.L. from the Spanish American Joint Committee for Scientific and Technological cooperation.

*Present address: Institute of High Energy Physics, Academia Sinica, Beijing, China.

[1] R. S. Bhalerao and L. C. Liu, Phys. Rev. Lett. **54**, 865 (1985).
[2] Q. Haider and L. C. Liu, Phys. Lett. B **172**, (1986) 257; **174**, 465(E) (1986).
[3] L. C. Liu and Q. Haider, Phys. Rev. C **34**, 1845 (1986).
[4] Li Yang-guo and H. C. Chiang, Nucl. Phys. **A454**, 720 (1986).
[5] G. L. Li, W. K. Cheng, and T. T. S. Kuo, Phys. Lett. B **195**, 515 (1987).
[6] R. E. Chrien *et al.*, Phys. Rev. Lett. **60**, 2595 (1988).
[7] B. J. Lieb *et al.* in Progress at LAMPF, 1988 (unpublished).
[8] E. Oset, H. Toki, and W. Weise, Phys. Rep. **83**, 281 (1982).
[9] M. Aguilar-Benitez *et al.*, Phys. Lett. B **204**, (1988).
[10] C. Itzykson and J. B. Zuber, *Quantum Field Theory* (McGraw-Hill, New York, 1980).
[11] R. M. Brown *et al.*, Nucl. Phys. **B153**, 89 (1979).
[12] C. B. Dover, J. Hüfner, and R. H. Lemmer, Ann. Phys. (N.Y.) **66**, 248 (1971).
[13] A. L. Fetter and J. D. Walecka, *Quantum Theory of Many*

Particle Systems (McGraw-Hill, New York, 1971).
[14] E. Oset and A. Palanques, Nucl. Phys. **A359**, 289 (1981).
[15] R. Machleidt, K. Holinde, and Ch. Elster, Phys. Rep. **149**, 1 (1987).
[16] G. E. Brown and A. D. Jackson, *The Nucleon-Nucleon Interaction* (North-Holland, Amsterdam, 1976).
[17] C. García-Recio, E. Oset, and L. L. Salcedo, Phys. Rev. C **37**, 194 (1988).
[18] E. Oset, Nucl. Phys. B **304**, 820 (1988).
[19] E. Hernández and E. Oset, Phys. Lett. B **184**, 1 (1987).
[20] E. Hernández and E. Oset, Nucl. Phys. **A493**, 453 (1989).
[21] L. Tauscher, C. García-Recio, and E. Oset, Nucl. Phys. **A415**, 333 (1984).
[22] E. Oset and L. L. Salcedo, Nucl. Phys. **A468**, 631 (1987).
[23] C. W. de Jager, C. de Vries, and H. de Vries, At. Data Nucl. Data Tables **14**, 480 (1974).
[24] L. L. Salcedo, E. Oset, M. J. Vicente-Vacas, and C. García-Recio, Nucl. Phys. **A484**, 557 (1988).
[25] M. J. López-Santodomingo, Tesina de Licenciatura (Universidad de Valladolid, 1985) (unpublished).
[26] E. Oset and L. L. Salcedo, J. Comput. Phys. **57**, 155 (1985).
[27] L. S. Kisslinger and W. L. Wang, Ann. Phys. (N.Y.) **99**, 374 (1976).
[28] A. N. Saharia and R. M. Woloshyn, Phys. Rev. C **21**, 1111 (1980).
[29] M. Hirata, F. Lenz, and K. Yazaki, Ann. Phys. (N.Y.) **108**, 16 (1977).
[30] E. Oset and W. Weise, Nucl. Phys. **A319**, 477 (1979).
[31] C. García-Recio, E. Oset, L. L. Salcedo, D. Strottman, and M. J. López, Nucl. Phys. (to be published).